# Nucleolar structure and function are regulated by the deubiquitylating enzyme USP36

**Akinori Endo[1], Masaki Matsumoto[2], Toshifumi Inada[3], Akitsugu Yamamoto[4], Keiichi I. Nakayama[2], Naomi Kitamura[1] and Masayuki Komada[1,*]**

[1]Department of Biological Sciences, Tokyo Institute of Technology, Yokohama 226-8501, Japan
[2]Department of Molecular and Cellular Biology, Medical Institute of Bioregulation, Kyushu University, Fukuoka 812-8582, Japan
[3]Department of Molecular Biology, Nagoya University, Nagoya 464-8602, Japan
[4]Department of Bio-science, Nagahama Institute of Bio-science and Technology, Nagahama 526-0829, Japan
*Author for correspondence (e-mail: makomada@bio.titech.ac.jp)

*Accepted 18 November 2008*
*Journal of Cell Science 122, 678-686 Published by The Company of Biologists 2009*
*doi:10.1242/jcs.044461*

## Summary

**The nucleolus is a subnuclear compartment and the site of ribosome biogenesis. Previous studies have implicated protein ubiquitylation in nucleolar activity. Here we show that USP36, a deubiquitylating enzyme of unknown function, regulates nucleolar activity in mammalian cells. USP36 localized to nucleoli via the C-terminal region, which contains basic amino acid stretches. Dominant-negative inhibition of USP36 caused the accumulation of ubiquitin-protein conjugates in nucleoli, suggesting that nucleoli are the site of USP36 action. USP36 deubiquitylated the nucleolar proteins nucleophosmin/B23 and fibrillarin, and stabilized them by counteracting ubiquitylation-mediated proteasomal degradation. RNAi-mediated depletion of cellular USP36 resulted in reduced levels of rRNA transcription and processing, a less-developed nucleolar morphology and a slight reduction in the cytoplasmic ribosome level, which eventually led to a reduced rate of cell proliferation. We conclude that by deubiquitylating various nucleolar substrate proteins including nucleophosmin/B23 and fibrillarin, USP36 plays a crucial role in regulating the structure and function of nucleoli.**

Supplementary material available online at
http://jcs.biologists.org/cgi/content/full/122/5/678/DC1

Key words: Deubiquitylating enzyme, Nucleolus, Protein degradation, Ribosome biogenesis, rRNA

## Introduction

Nucleoli are a subnuclear compartment located around the nucleolar organizer regions composed of gene clusters encoding rRNAs (Hernandez-Verdun, 2006; Raska et al., 2006). Nucleoli have a major role in ribosome biogenesis, where rRNAs are transcribed, processed and assembled with ribosomal proteins (r-proteins) to 60S and 40S ribosome subunits (Fatica and Tollervey, 2002; Tschochner and Hurt, 2003). Nucleoli also exert various non-ribosomal functions, including the regulation of cell-cycle and stress responses, as well as the processing and/or maturation of other non-coding RNA species (Boisvert et al., 2007).

Although the biological significance is not fully understood, substantial evidence implicates ubiquitin in nucleolar functions. Proteins in the rRNA processing machinery, such as nucleophosmin/B23 (NPM) and fibrillarin (FBRL), undergo ubiquitylation, which induces their proteasomal degradation (Chen et al., 2002; Itahana et al., 2003) or conversely, increases protein stability (Sato et al., 2004). Inhibition of proteasome activity causes deficient rRNA processing by affecting the nuclear distribution and mobility of rRNA-processing proteins (Stavreva et al., 2006). Other reports show that proteasomes and their potential target proteins are accumulated in nucleoli upon treatment with proteasome inhibitors, suggesting a role for nucleoli as a site of protein degradation (Mattsson et al., 2001; Arabi et al., 2003). In normal cells, however, proteasomes are excluded from nucleoli (Chen et al., 2002; Rockel et al., 2005). Ubiquitylation of r-proteins is also implicated in ribosome biogenesis. First, ubiquitin is partly translated as a fusion protein with the r-proteins L40 and S27a (Finley et al., 1989; Redman and Rechsteiner, 1989), which is required for efficient ribosome biogenesis (Finley et al., 1989). Second, r-protein L28 conjugated with Lys63-linked poly-ubiquitin is the major ubiquitylated protein in yeast cells, and the ubiquitylation might regulate the translation efficiency of ribosomes (Spence et al., 2000). The ubiquitylation of several other r-proteins has further been suggested by proteome analyses in both yeast and human cells (Peng et al., 2003; Matsumoto et al., 2005). Finally, proteome and live-cell imaging analyses of proteasome-inhibited human cells suggest that r-proteins that have failed to assemble into ribosome subunits in nucleoli are degraded by proteasomes (Andersen et al., 2005; Lam et al., 2007).

Ubiquitylation is a reversible modification, which is reverted by deubiquitylating enzymes (DUBs) that catalyze the cleavage of isopeptide bonding between target proteins and ubiquitin. The human genome encodes approximately 90 potential DUBs, and recent studies have elucidated important roles of protein deubiquitylation in regulating diverse ubiquitin-mediated cellular activities (Amerik and Hochstrasser, 2004; Nijman et al., 2005). DUBs are divided to five structurally distinct groups: ubiquitin-specific protease (USP), ubiquitin C-terminal hydrolase (UCH), ovarian tumor-related protease (OTU), Ataxin-3–Josephin and Jab1-MPN-Mov34 (JAMM) families (Amerik and Hochstrasser, 2004; Nijman et al., 2005). Whereas the JAMM family of DUBs are $Zn^{2+}$-containing metalloproteases, members of the other four families are Cys proteases, with conserved Cys and His boxes in the catalytic core. Among the five families, the USP family is the largest, comprising ~60 members in humans. USPs are multi-domain proteins which, in addition to the catalytic core, harbor regions with a unique domain composition, suggesting that different

USPs regulate different cellular functions by deubiquitylating unique substrate proteins at different subcellular sites.

Although our knowledge on the role of protein deubiquitylation has been expanding over the past few years, exact cellular functions of many individual DUBs remain unknown. In this study, we show that USP36, one of the uncharacterized DUBs of the USP family, has an essential role in maintaining the structure and function of nucleoli, providing a novel regulatory mechanism for nucleolar function.

## Results

### USP36 localizes to nucleoli

Although the DUB activity of USP36 has been detected in vivo and in vitro (Quesada et al., 2004; Kim et al., 2005), its cellular function is totally unknown. To elucidate it, we first determined the subcellular localization of USP36. When Flag-tagged human USP36 was expressed in HeLa cells and detected by immunocytochemistry, it localized to several intranuclear puncta, which were positive for a well-characterized antibody that diffusely stains nucleoli (e.g. Grandori et al., 2005) (Fig. 1A-A″).

To examine whether endogenous USP36 localizes to nucleoli, we generated an anti-USP36 antibody by immunizing rabbits with a unique C-terminal region of human USP36. Immunoblotting of HeLa cell lysate with the antibody, but not with the pre-immune serum, revealed a major band of ~125 kDa, with some smaller minor bands (Fig. 1B). The calculated molecular mass of human USP36 is 123 kDa, and the intensity of the ~125 kDa band increased when Flag-USP36 was overexpressed (Fig. 1C), indicating that the antibody primarily recognizes USP36 in the cells. Immunofluorescence with the antibody showed that endogenous USP36 also localizes to the nuclear puncta stained with the anti-nucleolus antibody in HeLa cells (Fig. 1D-D″). The puncta were also positive for nucleolar proteins, NPM (see Fig. 7C-C″) and fibrillarin (see Fig. 5B-B″). The second antiserum, raised in another rabbit, provided the same results, whereas pre-immune sera did not (data not shown). In addition, RNA interference (RNAi)-mediated USP36 depletion resulted in a loss of anti-USP36 staining in nucleoli (supplementary material Fig. S1).

Immuno-electron microscopy (immuno-EM) of HeLa cells with anti-USP36 antibody showed that the signals for endogenous USP36 (black dots) are concentrated and evenly distributed in nucleoli, which were observed as several electron-dense islands in the nucleus (Fig. 1E, arrowheads). In immuno-EM, subnucleolar structures were lost during the staining procedures because of the mild fixation conditions (compare with Fig. 7E). Pre-immune serum provided no nucleolar signals (data not shown).

### The C-terminal region targets USP36 to nucleoli

Other than the catalytic domain in the N-terminal region, USP36 contains no known domains. However, we found five stretches of Arg and Lys residues in its C-terminal region (Fig. 2A), which potentially serve as the nucleolar localization signal (NoLS) (e.g. Valdez et al., 1994; Horke et al., 2004) or nuclear localization signal (NLS) (Jans et al., 2000). To determine the region of USP36 responsible for its nucleolar localization, we divided the protein into three parts: the N-terminal region containing the catalytic domain (residues 1-420), the central region (residues 421-800) and the C-terminal region containing all the basic stretches (residues 801-1121) (Fig. 2A,B). When tagged with the Flag epitope and expressed in HeLa cells, these mutants exhibited different subcellular localization: USP36$^{1\text{-}420}$ mainly distributed to the cytoplasm (Fig. 2C-C″), USP36$^{421\text{-}800}$ to the nucleoplasm (Fig. 2D-D″) and USP36$^{801\text{-}1121}$ to nucleoli (Fig. 2E-E″). Deletion of the C-terminal region from full-length USP36 (Fig. 2A,B) (Δ801-1121) also caused mislocalization of the protein to the nucleoplasm (Fig. 2F-F″). These results suggest that the NoLS lies in the C-terminal region of USP36.

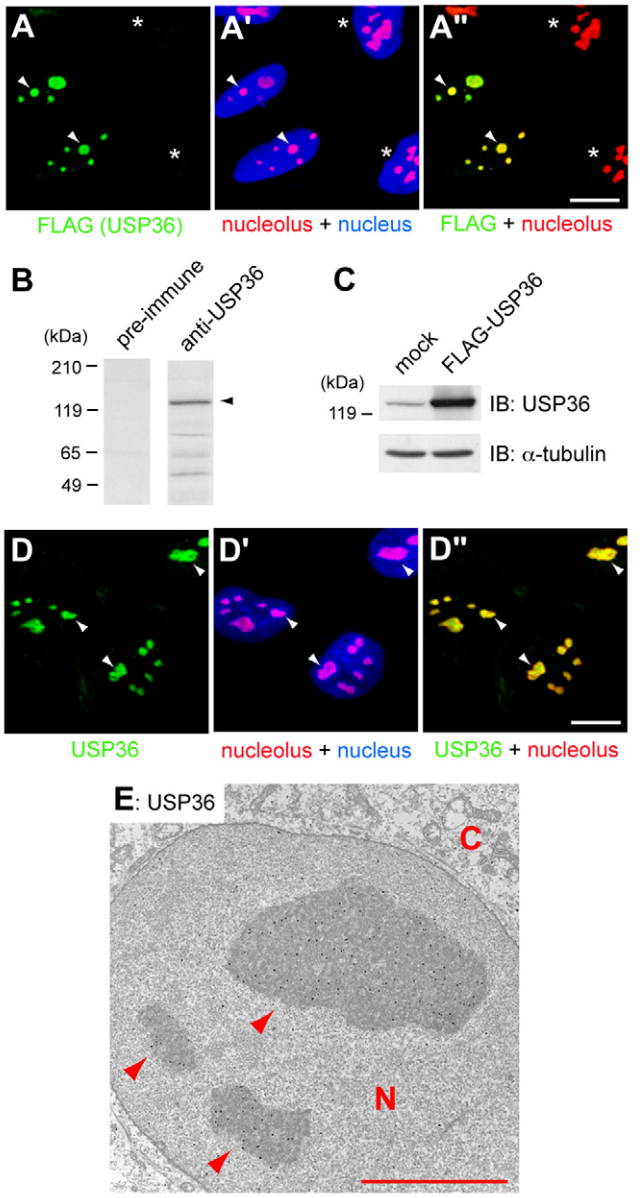


**Fig. 1.** USP36 localizes to nucleoli. (A-A″) HeLa cells were transfected with Flag-USP36, and double-stained with anti-Flag (A) and anti-nucleolus (A′, red) antibodies. In A′, nuclei were also stained in blue. A″ is the merged image. Arrowheads indicate typical nucleoli. Asterisks indicate untransfected cells. Scale bar: 10 μm. (B) HeLa cell lysate immunoblotted with pre-immune serum or anti-USP36 antiserum. Arrowhead indicates full-length USP36. (C) Lysates of HeLa cells transfected with or without Flag-USP36 immunoblotted with anti-USP36 and anti-α-tubulin antibodies. (D-D″) HeLa cells double-stained with anti-USP36 (D) and anti-nucleolus (D′, red) antibodies. D″ is the merged image. Arrowheads indicate typical nucleoli. Scale bar: 10 μm. (E) Immuno-EM analysis of HeLa cells with anti-USP36 antibody. Nucleoli are indicated by arrowheads. N and C indicate the nucleoplasm and cytoplasm, respectively. Scale bar: 5 μm.

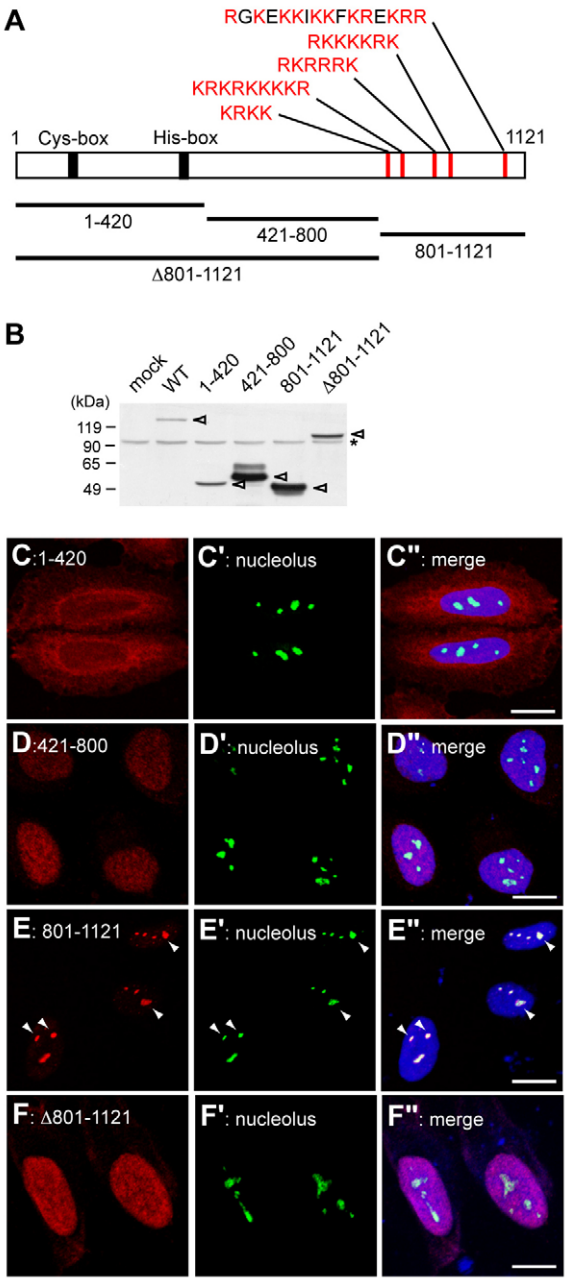


**Fig. 2.** The C-terminal region targets USP36 to nucleoli. (A) Schematic structure of human USP36. Five basic stretches in the C-terminal region, as well as the Cys and His boxes, are indicated. Regions covered by the four truncated mutants used in this study are also shown. (B) Lysates of HeLa cells transfected with Flag-tagged wild-type and truncated USP36 constructs were immunoblotted with anti-Flag antibody. Open arrowheads and asterisk indicate the USP36 constructs and a non-specific band, respectively. (C-F″) HeLa cells were transfected with Flag-tagged USP36$^{1\text{-}420}$ (C-C″), USP36$^{421\text{-}800}$ (D-D″), USP36$^{801\text{-}1121}$ (E-E″) or USP36$^{\Delta 801\text{-}1121}$ (F-F″), and double-stained with anti-Flag (C-F) and anti-nucleolus (C′-F′) antibodies. C″-F″ are merged images in which nuclei were also stained in blue. Arrowheads in E-E″ indicate typical nucleoli. Scale bars: 10 μm.

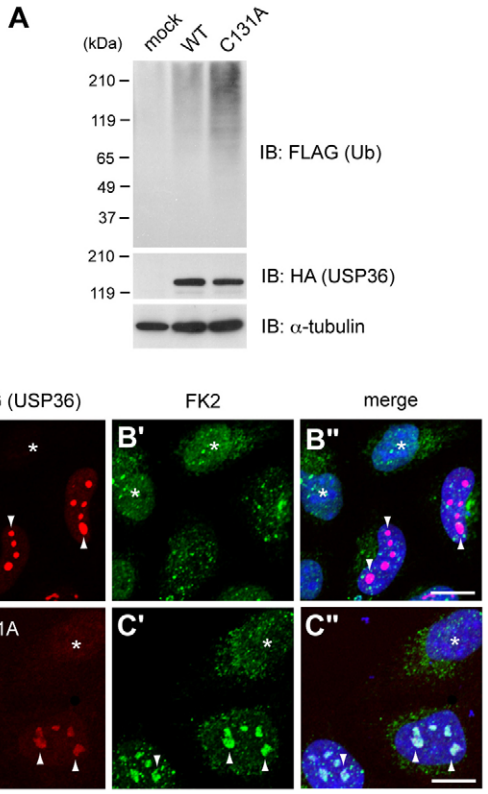


**Fig. 3.** USP36 exhibits DUB activity in nucleoli. (A) COS-7 cells were transfected with HA-tagged wild-type USP36 or USP36$^{C131A}$ together with Flag-ubiquitin for 2 days, and treated with MG132 for 8 hours. Their lysates were immunoblotted with anti-Flag, anti-HA and anti-α-tubulin antibodies. (B-C″) HeLa cells transfected with Flag-tagged wild-type USP36 (B-B″) or USP36$^{C131A}$ (C-C″) and double-stained with anti-Flag (B,C) and FK2 (B′,C′) antibodies. B″ and C″ are merged images. Arrowheads indicate typical nucleoli. Asterisks indicate untransfected cells. Scale bars: 10 μm.

## USP36 exhibits DUB activity in nucleoli

We next examined the effect of overexpressing wild-type or catalytically inactive USP36 on cellular ubiquitylation. As a common method to inactivate Cys proteases, we introduced a Cys-to-Ala mutation in the active site Cys131 residue within the Cys-box of USP36. COS-7 cells were transfected with HA-tagged wild-type USP36 or USP36$^{C131A}$, together with Flag-tagged ubiquitin. Cells were harvested after treatment with the proteasome inhibitor MG132, and lysates were immunoblotted with anti-Flag antibody to detect the ubiquitylation of cellular proteins. Overexpression of USP36$^{C131A}$ resulted in a significant increase in the level of protein ubiquitylation in the cells (Fig. 3A), This suggests that USP36$^{C131A}$ inhibits endogenous USP36 activity in a dominant-negative manner and that the accumulated ubiquitylated proteins in USP36$^{C131A}$-expressing cells are potential USP36 substrates, which remain ubiquitylated when the USP36 activity is inhibited. Overexpression of wild-type USP36 also raised the level of protein ubiquitylation, although only slightly (Fig. 3A). This might be a secondary effect of USP36 overexpression that somehow resulted in the functional disorganization of nucleoli.

To determine the subcellular site where ubiquitylated proteins accumulate in USP36$^{C131A}$-expressing cells, we immunofluorescently stained USP36$^{C131A}$-transfected HeLa cells with FK2, an anti-ubiquitin antibody that recognizes ubiquitin only when it is conjugated to other proteins, including ubiquitin (Fujimuro and Yokosawa, 2005). In addition to the low background staining in the nucleus and cytoplasm, FK2 stained Flag-USP36$^{C131A}$-positive nucleoli (Fig. 3C-C″). The nucleolar staining

was not observed in untransfected (Fig. 3B-B″,C-C″, asterisks) and wild-type USP36-expressing (Fig. 3B-B″) cells. Collectively, these results suggest that nucleoli are a major site of USP36-mediated protein deubiquitylation.

### Proteome analysis identifies NPM and fibrillarin as USP36 substrates

To identify substrate proteins for USP36, we performed a proteome analysis of ubiquitylated proteins that accumulated in USP36$^{C131A}$-expressing cells. Nuclei were isolated from mock- and USP36$^{C131A}$-transfected HeLa cells. Proteins were extracted from nuclei and separated using anti-ubiquitin affinity chromatography using FK2. Ubiquitylated proteins were eluted from the affinity column, trypsinized, and subjected to liquid chromatography tandem mass spectrometry (MS). This experiment identified peptides corresponding to 278 and 365 proteins from mock- and USP36$^{C131A}$-transfected cells, respectively (data not shown). Most proteins identified in mock-transfected cells were also identified in USP36$^{C131A}$-transfected cells. Among them, three human NPM peptides were identified from USP36$^{C131A}$-transfected cells: $^{33}$VDNDENEHQLSLR$^{45}$ (3 hits, MASCOT score=41~64), $^{55}$DELHIVEAEAMNYEGSPIK$^{73}$ (1 hit, MASCOT score=43) and $^{80}$MSVQPTVSLGGFEITPPVVLR$^{101}$ (3 hits, MASCOT score=51~64). Only $^{33}$VDNDENEHQLSLR$^{45}$ (2 hits, MASCOT score=52~58) was identified from mock-transfected cells. A peptide corresponding to $^{305}$DHAVVVGVYRPPPK$^{318}$ in human fibrillarin (1 hit, MASCOT score=43) was also identified from USP36$^{C131A}$-transfected cells but was not found in mock-transfected cells. In this study, we focused on NPM and fibrillarin because these proteins localize to nucleoli and have been shown to undergo ubiquitylation (Chen et al., 2002; Itahana et al., 2003; Sato et al., 2004).

### USP36 deubiquitylates and stabilizes NPM

We first examined USP36-mediated deubiquitylation of NPM. COS-7 cells were transfected with HA-tagged wild-type USP36 or USP36$^{C131A}$, together with Flag-ubiquitin, and treated with MG132. Endogenous NPM was immunoprecipitated from the cells, and immunoblotted with anti-Flag antibody to detect ubiquitylation. Expression of USP36$^{C131A}$ significantly elevated the level of a >50 kDa smear, which represents polyubiquitylated NPM (Fig. 4A, top, asterisk). Expression of wild-type USP36, by contrast, only slightly elevated the level of NPM ubiquitylation (Fig. 4A, top). Together with the observation that USP36 and NPM colocalize in nucleoli (Fig. 7C-C″), these results suggested that NPM is a cellular substrate for USP36. In addition, when HA-tagged USP36 and USP36$^{C131A}$ were immunoprecipitated from the cells, both proteins co-precipitated endogenous NPM, suggesting that USP36 stably interacts with NPM in vivo (Fig. 4B, top).

To test whether deubiquitylation regulates the stability of NPM protein by removing the proteasomal degradation signal, we constructed two small interfering RNA (siRNA) expression vectors for human USP36, and transfected them into HeLa cells. In siRNA-transfected cells, the level of USP36 expression was reduced (Fig. 4C, middle), and concomitantly, the level of NPM was also reduced (Fig. 4C, top), suggesting that USP36 stabilizes NPM by counteracting ubiquitin-dependent degradation.

### USP36 deubiquitylates and stabilizes fibrillarin

We next examined the deubiquitylation of fibrillarin. COS-7 cells were transfected with Flag-tagged fibrillarin together with HA-tagged USP36 or USP36$^{C131A}$, and treated with MG132. Flag-fibrillarin was immunoprecipitated from the cells and immunoblotted with the anti-ubiquitin antibody FK2. In the precipitate from USP36$^{C131A}$-transfected cells, FK2 detected a major band corresponding to monoubiquitylated fibrillarin (Fig. 5A, top, open arrowhead) as well as a faint higher-molecular-mass smear (Fig. 5A, top, asterisk). These fibrillarin bands were detected at much lower levels in mock-transfected cells, and disappeared when wild-type USP36 was overexpressed (Fig. 5A, top). In addition, Flag-fibrillarin colocalized with endogenous USP36 in nucleoli in immunofluorescence (Fig. 5B-B″).

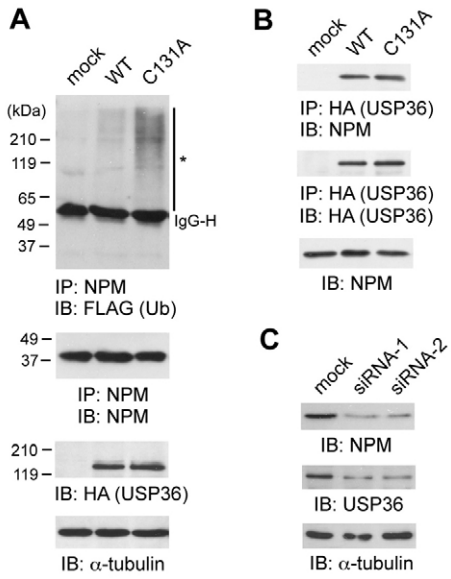


**Fig. 4.** USP36 deubiquitylates and stabilizes NPM. (A) COS-7 cells transfected with HA-tagged wild-type USP36 or USP36$^{C131A}$ with Flag-ubiquitin for 2 days, and treated with MG132 for 8 hours. Lysates were immunoprecipitated with anti-NPM antibody and immunoblotted with anti-Flag (top) and anti-NPM (second from top) antibodies. Expression levels of HA-tagged USP36 constructs and endogenous α-tubulin (loading control) assessed by immunoblotting of the total cell lysates with anti-HA (third from top) and anti-α-tubulin (bottom) antibodies. Asterisk indicates the smear of polyubiquitylated NPM. (B) Lysates of COS-7 cells transfected with HA-tagged wild-type USP36 or USP36$^{C131A}$ immunoprecipitated with anti-HA antibody and immunoblotted with anti-NPM (top) and anti-HA (middle) antibodies. Expression levels of NPM were assessed by immunoblotting of the total cell lysates with anti-NPM antibody (bottom). (C) Lysates of HeLa cells transfected with the mock or USP36 siRNA vectors were immunoblotted with anti-NPM, anti-USP36 and anti-α-tubulin antibodies.

We next examined the effect of USP36 overexpression on fibrillarin protein stability. COS-7 cells were transfected with Flag-fibrillarin, with or without HA-USP36, and chased in the presence of cycloheximide (CHX) for 24 and 36 hours. Although Flag-fibrillarin was gradually degraded in mock-transfected cells, substantial amounts of the protein were detected even after a 36-hour chase in USP36-overexpressing cells (Fig. 5C, top). Collectively, these results suggest that USP36 also deubiquitylates and stabilizes fibrillarin.

### USP36 is required for cell proliferation

During experiments using USP36 siRNAs, we noticed that the siRNA-transfected cells proliferated much more slowly than mock-transfected cells. To confirm this effect in a quantitative manner, the same number of HeLa cells were transfected with the mock or USP36 siRNA vectors for 6 days, trypsinized, and counted using

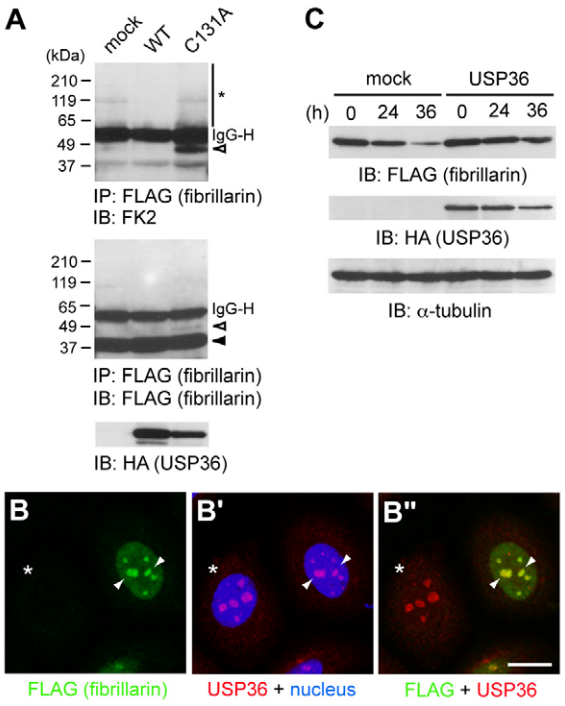


**Fig. 5.** USP36 deubiquitylates and stabilizes fibrillarin. (A) COS-7 cells transfected with Flag-fibrillarin with HA-tagged wild-type USP36 or USP36$^{C131A}$ for 2 days, and treated with MG132 for 8 hours. Their lysates were immunoprecipitated with anti-Flag antibody and immunoblotted with FK2 (top) and anti-Flag (middle) antibodies. Closed arrowhead, open arrowhead and asterisk indicate non-, mono- and poly-ubiquitylated fibrillarin, respectively. Expression levels of the HA-USP36 constructs were assessed by immunoblotting of the total cell lysates with anti-HA antibody (bottom). (B-B″) HeLa cells transfected with Flag-fibrillarin and double-stained with anti-Flag (B) and anti-USP36 (B′, red) antibodies. B″ is the merged image. Arrowheads indicate typical nucleoli. Asterisks indicate untransfected cells. Scale bar: 10 μm. (C) COS-7 cells transfected with Flag-fibrillarin with or without HA-USP36 for 2 days, and further cultured in the presence of CHX for 24 or 36 hours. Lysates of the cells were immunoblotted with anti-Flag, anti-HA and anti-α-tubulin antibodies.

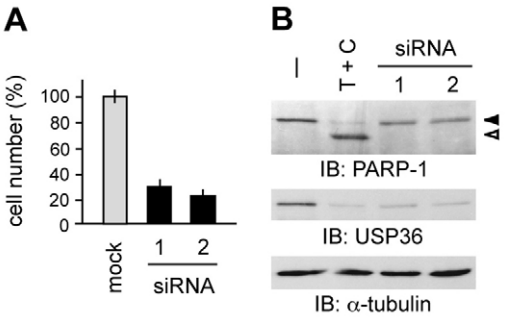


**Fig. 6.** USP36 is required for normal cell proliferation. (A) An equal number of HeLa cells were transfected with the mock or USP36 siRNA vectors for 6 days, trypsinized and the cell number counted. The relative number of siRNA-transfected cells compared with that of mock-transfected cells is shown as a percentage. Mean ± s.d. of a typical triplicate experiment is shown. (B) HeLa cells were treated with or without TNF-α and CHX (T + C) or transfected with USP36 siRNAs. Their lysates were immunoblotted with anti-PARP1, anti-USP36 and anti-α-tubulin antibodies. Closed and open arrowheads indicate uncleaved and cleaved PARP1, respectively. The reason for the reduced USP36 expression after treatment with TNFα and CHX is unclear.

a hemocytometer. Fig. 6A shows results of a typical triplicate experiment. Transfection of either USP36 siRNA caused a 70-80% reduction in the cell number compared with mock transfection.

Transfection of USP36 siRNAs did not cause fragmentation of cells and nuclei (supplementary material Fig. S1), suggesting that USP36 depletion does not induce apoptosis. To confirm this, we examined the caspase-mediated cleavage of poly(ADP-ribose) polymerase-1 (PARP1), an established marker of apoptosis. In control cells in which apoptosis was induced by tumor necrosis factor-α (TNFα) and CHX, PARP1 was processed from a 113 kDa precursor to the mature 89 kDa form (Fig. 6B, top). Such cleavage did not occur in USP36-depleted cells (Fig. 6B, top), suggesting that the reduced cell number in the USP36-depleted conditions is due not to cell death, but to a reduced rate of cell proliferation.

## USP36 is required for a normal nucleolar structure

To elucidate the primary defect leading to the reduced proliferation of USP36-depleted cells, we examined the effect of USP36 RNAi on the structure and function of nucleoli. We first examined nucleolar morphology by immunocytochemistry. HeLa cells were transfected with the mock or USP36 siRNA vectors, and double-stained with anti-nucleolus and anti-USP36 antibodies. When siRNAs were transfected, nucleolar anti-USP36 staining was lost in ~50% of the cells (supplementary material Fig. S1). In such cells, anti-nucleolus antibody exhibited nearly undetectable levels of nucleolar staining (Fig. 7A-A″, asterisks), or stained much smaller dots than those in control nucleoli (Fig. 7B-B″, asterisk). Anti-NPM antibody stained nuclei, with an especially high level of staining at nucleoli, in control cells (Fig. 7C-C″). In USP36 siRNA-transfected cells, by contrast, a punctate nucleolar localization of NPM was hardly detectable, and concomitantly, its nucleoplasmic level increased (Fig. 7D-D″), consistent with the observation that nucleoli are lost in the siRNA-transfected cells (Fig. 7A-B″).

The absence of normal nucleolar morphology in USP36-depleted cells was confirmed by EM. Nucleoli, composed of the fibrillar center, dense fibrillar component and granular component, were observed in mock-transfected cells (Fig. 7E, arrowheads and inset). In siRNA-transfected cells, the size of the nucleoli was much smaller than that in control cells (Fig. 7F, arrowhead). The subnucleolar structures, however, appeared to be retained in the remnants (Fig. 7F, inset). Together with the immunofluorescence data (Fig. 7A-D″), these results indicated that the nucleolar structure itself is not well developed in USP36-depleted cells.

## USP36 is required for rRNA transcription and processing

Nucleoli are the sites of rRNA transcription and processing. To test whether USP36-depleted cells retain these activities, we examined the rate of rRNA transcription and processing in pulse-labeling experiments. Mock- and USP36-siRNA-transfected HeLa cells were metabolically labeled with [$^{32}$P]orthophosphate for 45 minutes, and chased in the absence of [$^{32}$P]orthophosphate for 30 and 90 minutes. Total RNA isolated from an equal number of cells was separated by electrophoresis, and labeled rRNAs were visualized by autoradiography after transfer to a nylon membrane (Fig. 8A, top). The amount of $^{32}$P incorporated into 47S pre-rRNA was reduced in USP36 siRNA-transfected cells, suggesting that rRNA transcription is impaired by USP36 depletion (Fig. 8A, top, 0 minutes). However, staining of the membrane with methylene blue showed the total cellular levels of 28S and 18S rRNAs to be similar in mock- and siRNA-transfected cells (Fig. 8A, bottom). This is

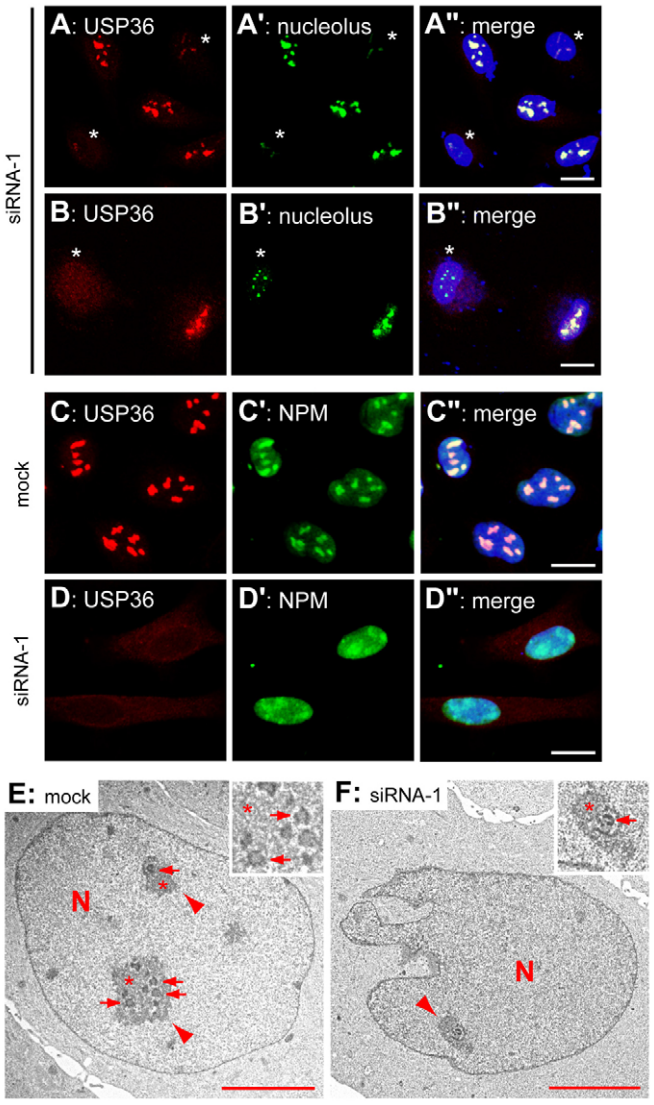


**Fig. 7.** USP36 is required for a normal nucleolar structure. (A-D″) HeLa cells transfected with the USP36 siRNA-1 (A-A″, B-B″, and D-D″) or mock (C-C″) vector and stained with anti-USP36 antibody (A-D) with anti-nucleolus (A′,B′) or anti-NPM (C′,D′) antibody. A″-D″ are merged images. Asterisks in A-A″ and B-B″ indicate USP36-depleted cells. Scale bars: 10 µm. (E,F) EM of HeLa cells transfected with mock vector (E) or USP36 siRNA-1 vector (F). N and arrowheads indicate the nucleoplasm and nucleoli, respectively. Insets show high-magnification images of the nucleoli. In nucleoli, the granular components (asterisks), and the dense fibrillar components (arrows) surrounding the fibrillar center, are indicated. Scale bars: 5 µm.

suggestive of a checkpoint control system for rRNA biogenesis (see below).

47S pre-rRNA is processed via 32S pre-rRNA to 28S, 18S and 5.8S rRNAs (Fatica and Tollervey, 2002; Tschochner and Hurt, 2003). After the chase for 30 and 90 minutes, the amounts of all the processed rRNAs increased in both mock- and USP36-siRNA-transfected cells (Fig. 8A, top). Quantification of the radioactivity of the rRNA bands, however, showed that USP36 depletion caused a delay in rRNA processing (Fig. 8B). In siRNA-transfected cells compared with mock-transfected cells, the ratio of 32S rRNA to 47S rRNA was already lower before the chase (0 minutes), and those of 28S and 18S rRNAs to 47S rRNA were significantly lower after the 30-minute chase. These ratios returned to an almost normal level after 90 minutes of chase. The ratio of 5S or 5.8S rRNAs to 47S rRNA was much lower, even after the 90-minute chase, in siRNA-transfected cells.

### USP36 is required for efficient ribosome biogenesis

To test whether the reduced rate of rRNA biogenesis affects the amount of cytoplasmic ribosomes in USP36-depleted cells, we performed a ribosome-profiling experiment. HeLa cells were transfected with the mock or USP36 siRNA vectors and cytoplasmic fractions were prepared from an equal number of cells. Ribosome profiling of the cytoplasmic fractions using sucrose density gradient centrifugation showed that the amount of mature 80S ribosomes was reproducibly reduced by 13-30% upon siRNA transfection (Fig. 8C). These results must be an underestimate because USP36 was efficiently depleted in ~50% of siRNA-transfected cells, suggesting that USP36 is required for maximal ribosome biogenesis. The levels of the 60S and 40S ribosome subunits as well as polysomes were difficult to compare because they were much lower than levels of 80S ribosomes, but they did not differ significantly between mock- and siRNA-transfected cells (Fig. 8C).

## Discussion

Although ubiquitylation has been implicated in several aspects of nucleolar function, its biological significance has been unclear. In this study, we describe a novel regulatory mechanism for nucleolar structure and function which is mediated by USP36, a DUB of the USP family. Our results provide direct evidence of an essential role for protein deubiquitylation, and therefore ubiquitylation, in the regulation of nucleolar function. Possible orthologs of mammalian USP36 are found in the zebrafish and fruit fly but not in the yeast or nematode, suggesting that such a regulation is acquired during the evolution of higher eukaryotes.

### Subcellular localization of USP36

For DUBs, as for other enzymes, subcellular localization has a crucial role in determining substrate specificity in vivo. We showed that USP36 specifically localizes to nucleoli (Fig. 1). This is so far the only DUB that exhibits nucleolar localization. Nucleoli are compartmentalized into three sub-regions: the fibrillar center, the dense fibrillar component and the granular component (Hernandez-Verdun, 2006; Raska et al., 2006). NPM and fibrillarin localize to the granular component and the dense fibrillar component, respectively, and participate in different steps of rRNA processing (Boisvert et al., 2007). Consistent with the observations that USP36 deubiquitylates NPM and fibrillarin (Figs 4, 5), USP36 colocalized with both these proteins (Figs 5 and 7). Together with the scattered nucleolar localization pattern of USP36 observed by immuno-EM (Fig. 1), these results suggest that USP36 functions diffusely in nucleoli.

Although no consensus sequences have been identified, short stretches of basic amino acids have been identified as NoLSs for various nucleolar proteins. They are similar to conventional NLSs recognized by importin proteins (Jans et al., 2000), but have been reported to interact with rRNA (Gustafson et al., 1998) or the acidic regions of NPM (Adachi et al., 1993). The C-terminal region of USP36 contains five clusters of Arg and Lys residues, and was necessary and sufficient for the nucleolar localization of USP36 (Fig. 2). These results indicate that the C-terminal region harbors the NoLS, and suggest that one (or some) of the basic stretches serves as the NoLS, which might interact with NPM (Fig. 4) or

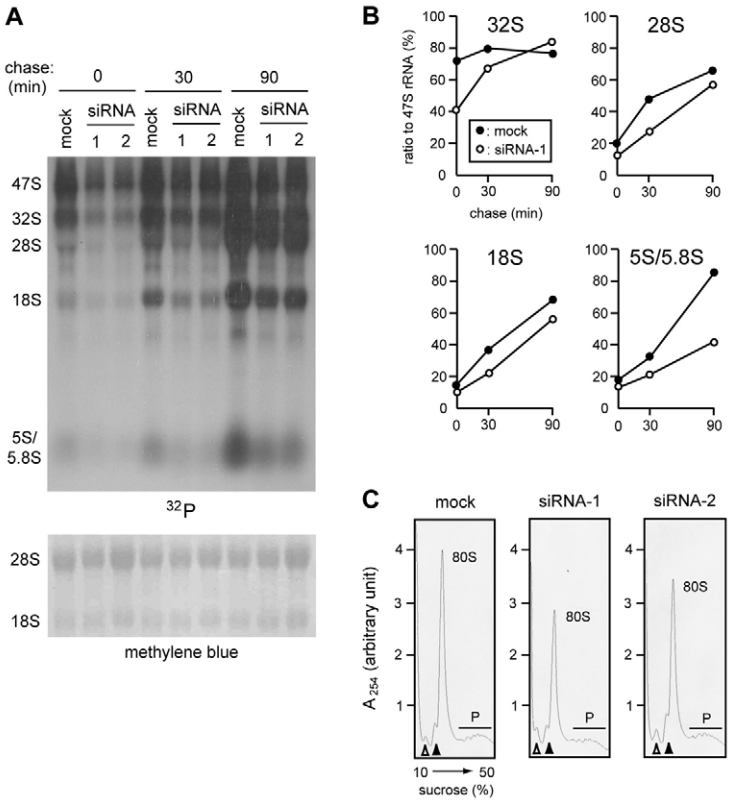


**Fig. 8.** USP36 is required for biogenesis of rRNAs and ribosomes. (A) HeLa cells transfected with the mock or USP36 siRNA vectors incubated in the presence of [$^{32}$P]orthophosphate for 45 minutes, and chased in the absence of [$^{32}$P]orthophosphate for 30 or 90 minutes. Total RNA was isolated from an equal number of cells, separated by electrophoresis, and transferred to a nylon membrane. The membrane was exposed to X-ray film (top) or stained with methylene blue (bottom). The levels of $^{32}$P-labeled rRNAs increased during the chasing period, probably because intracellularly incorporated [$^{32}$P]orthophosphate cannot be removed by rinsing with PBS. (B) Quantification of radioactivity of rRNAs in mock- and USP36 siRNA-1-transfected cells in A. The ratio of each processed rRNA to 47S pre-RNA is shown as a percentage. Closed circles, mock; open circles, USP36 siRNA-1. (C) HeLa cells were transfected with the mock or USP36 siRNA vectors, and cytoplasmic fractions were prepared from an equal number of cells. The fractions were subjected to 10-50% sucrose density gradient centrifugation and fractionated, and RNA was detected by measuring absorbance at 254 nm ($A_{254}$). Positions of the 80S ribosome, 60S (closed arrowhead) and 40S (open arrowhead) ribosome subunits, and polysomes (P) are indicated.

rRNA. Some nucleolar proteins harbor an NoLS and an NLS, both of which are required for correct nucleolar localization (Valdez et al., 1994; Hahn and Marsh, 2007). Therefore, it is possible that one of the basic stretches serves as the NoLS while another serves as the NLS. Moreover, there might be an additional NLS in the central region because USP36$^{421\text{-}800}$ localized to the nucleoplasm (Fig. 2).

### Substrate proteins for USP36

We showed that NPM and fibrillarin, two nucleolar proteins that have previously been shown to undergo ubiquitylation, are substrates for USP36 (Figs 4 and 5). The level of NPM decreased when cellular USP36 was depleted using RNAi, and the rate of fibrillarin degradation decreased upon overexpression of wild-type USP36 (Figs 4 and 5). These results suggest a regulatory role of USP36 that counteracts ubiquitylation-mediated protein degradation. Namely, USP36 stabilizes these proteins by removing the proteasome-targeting signal and preventing their degradation. In addition to proteasomal degradation, however, ubiquitylation is involved in various other cellular events, such as endocytic protein sorting, DNA repair and r-protein function (Spence et al., 2000; Haglund and Dikic, 2005). Therefore, another possibility, that deubiquitylation regulates the proteins in different ways, cannot be ruled out. Consistent with the fact that both NPM and fibrillarin participate in rRNA processing, the rate of rRNA processing was reduced by USP36 depletion (Fig. 8). Although USP36 siRNAs only delayed, but did not inhibit, rRNA processing, the results might not fully reflect the effect of USP36 depletion for the following reason. As the knockdown efficiency of the USP36 siRNA vectors was relatively low (~50%), processing of rRNA detected in siRNA-transfected cells might correspond to that in cells in which efficient depletion of USP36 failed. In cells that are successfully depleted of USP36, processing of 47S rRNA might not be detectable because its transcription is already inhibited in such cells (Fig. 8).

The reduced rate of rRNA transcription in USP36-depleted cells raises the possibility that the stability of proteins in the rRNA transcription machinery is also regulated by USP36. The rRNA transcription machinery is a large protein complex including RNA polymerase I, upstream binding factor UBF and selectivity factor SL1 (Hernandez-Verdun et al., 2002). None of these, however, was identified as a potential substrate of USP36 in our proteome analysis (data not shown). The mechanism by which USP36 regulates rRNA transcription remains to be elucidated.

Several r-proteins have been shown to undergo ubiquitylation (Spence et al., 2000; Peng et al., 2003; Matsumoto et al., 2005). In addition, inhibition of the proteasome activity results in the accumulation of r-proteins in nucleoli, suggesting that r-proteins that have failed to assemble into ribosome subunits undergo proteasomal degradation (Andersen et al., 2005; Lam et al., 2007). Our proteome analysis identified a number of r-proteins as possible substrates of USP36 (data not shown). These results need to be evaluated with caution because in proteome analyses, r-proteins have often been detected non-specifically due to their abundance in the cell (Blagoev et al., 2003) (M.M. and K.I.N., unpublished data). Nevertheless, it is possible that the degradation and stability of r-proteins are also regulated by USP36-mediated deubiquitylation. The slight reduction in the level of cytoplasmic 80S ribosomes caused by USP36 depletion (Fig. 8) might support this notion. This is another important issue that remains to be addressed.

### Cellular function of USP36

In USP36-depleted cells, rRNA transcription and processing were affected and the normal nucleolar structure was lost (Figs 7 and 8). Concomitantly, the proliferation of USP36-depleted cells was

severely inhibited (Fig. 6). It is therefore possible that the deficient nucleolar function led to reduced translation capacity because of a shortage of ribosomes, which resulted in the proliferation defect in USP36-depleted cells. However, the only slightly reduced level of ribosomes shown in Fig. 8 might not be sufficient to affect cell proliferation. Cellular levels of 28S and 18S rRNAs were not apparently reduced by USP36 depletion either (Fig. 8). Several studies in yeast and human cells have suggested a checkpoint control system that senses the cellular activity to newly synthesize ribosomes, independently of the level of pre-existing ribosomes (Oeffinger and Tollervey, 2003; Zhang et al., 2003; Bernstein et al., 2007). Another even more likely possibility, therefore, is that cells stalled in cell division when they were deficient in ribosome biogenesis in the absence of USP36.

Nucleoli are disassembled during mitosis and reassembled after mitosis. For the post-mitotic nucleolar assembly, RNA-polymerase-I-mediated rRNA transcription at the nucleolar organizer region is prerequisite (Hernandez-Verdun et al., 2002). Once rRNA is transcribed, proteins of the rRNA-processing machinery are relocated from the prenucleolar body to the nucleolar-organizer region to promote further ribosome biogenesis, which results in the formation of the nucleolar structure (Hernandez-Verdun et al., 2002). In USP36-depleted cells, the rate of 47S pre-rRNA transcription and processing was reduced (Fig. 8) and the levels of prenucleolar body proteins, NPM and fibrillarin, were downregulated (Figs 4 and 5). We therefore propose that the primary role of USP36 is to regulate the transcription and processing of rRNA by deubiquitylating various proteins involved in these processes, and the aberrant nucleolar structure in its absence is secondary to deficient ribosome biogenesis. This is supported by a previous observation that similar disruption of the nucleolar structure is caused by knockout of the gene encoding TIF-IA (*Trim24*), a component of the rRNA transcription machinery, in mice (Yuan et al., 2005).

The level of ribosomes, which determines the translational capacity of the cell, undergoes tight regulation by extracellular stimuli such as nutrient availability, growth factors and stress. RNA-polymerase-I-dependent rRNA transcription is believed to have a central role in this regulation (Grummt, 1999). Our results suggest that in addition to the transcriptional regulation, USP36-mediated deubiquitylation serves as a novel mechanism that dynamically regulates the ribosome activity in response to changes in environmental conditions.

## Materials and Methods

### Anti-USP36 antisera

A C-terminal unique region of human USP36 (residues 921 to 1121) was cloned into the vector pGEX6P-2 (GE Healthcare, Piscataway, NJ) to generate a glutathione *S*-transferase fusion construct. The fusion protein was purified from *Escherichia coli* cells using glutathione-Sepharose affinity beads (GE Healthcare) and 200 μg protein was used to immunize each rabbit. Antisera were raised in two rabbits.

### Expression constructs and DNA transfection

Human cDNAs for USP36 and fibrillarin were obtained from Kazusa DNA Research Institute (Kisarazu, Japan) and Open Biosystems (Huntsville, AL), respectively, and cloned into the mammalian expression vectors, pME-Flag and pME-HA. The cDNA for USP36$^{C131A}$ was generated using the QuikChange site-directed mutagenesis system (Stratagene, La Jolla, CA). cDNAs for truncated USP36 mutants were amplified from the full-length cDNA by PCR. The Flag-ubiquitin expression vector was provided by Toshiaki Suzuki (Tokyo Metropolitan Institute of Medical Science, Tokyo, Japan). Expression vectors were transfected into cells for 2 days using the FuGENE6 Transfection Reagent (Roche Diagnostics, Indianapolis, IN).

### RNAi

Two siRNA expression vectors for human USP36 were constructed using the vector pSilencer 1.0-U6 (Ambion, Austin, TX). The mRNA target sites were nucleotides 1276-1294 (5′-CGTATATGTCCCAGAATAA-3′) and 3065-3083 (5′-GGAAGA-GTCTCCAAGGAAA-3′) from the translation initiation codon for siRNA-1 and siRNA-2, respectively. These vectors or an empty mock vector were transfected into cells three times at 48-hour intervals. Before the second and third rounds of transfection, cells were trypsinized and re-seeded at low density to avoid confluent culture.

### Immunoprecipitation and immunoblotting

Cell lysates were prepared by solubilizing cells in 50 mM Tris-HCl, pH 7.4, 150 mM NaCl, 0.1% Tween-20, 1 mM EDTA, 10 mM N-ethylmaleimide, 50 mM NaF, 30 mM sodium pyrophosphate, 1 mM $Na_3VO_4$, and protease inhibitor cocktail (1 mM phenymethyl sulfonyl fluoride, 1 μg/ml aprotinin, 1 μg/ml leupeptin and 1 μg/ml pepstatin A) for 30 minutes on ice and collecting the supernatant after centrifugation at 12,000 ***g*** for 15 minutes at 4°C. The lysates were directly used for immunoblotting, or immunoprecipitated with anti-Flag M2 (1 μg, Sigma, St Louis, MO), anti-HA 12CA5 (3 μg, Roche Diagnostics) or anti-NPM (3 μg, Zymed Laboratories, South San Francisco, CA) antibody. Immunoblotting was performed using standard procedures. Primary antibodies were anti-USP36 (1:100), anti-Flag M2 (4 μg/ml), anti-HA 12CA5 (0.4 μg/ml), anti-ubiquitin (5 μg/ml, FK2, MBL, Nagoya, Japan), anti-NPM (2 μg/ml), anti-α-tubulin (1:20,000; Sigma), and anti-PARP1 (1:1000; Cell Signaling Technology, Danvers, MA) antibodies. Secondary antibodies were peroxidase-conjugated anti-mouse IgG and anti-rabbit IgG antibodies (GE Healthcare). Blots were detected using the ECL reagent (GE Healthcare). Where described, cells were treated with 5 μM CHX or 20 μM MG132 for the indicated duration prior to lysis. To induce apoptosis, cells were treated with TNF-α (20 ng/ml, provided by Masafumi Tsujimoto, RIKEN, Wako, Japan) and 0.36 mM CHX for 4 hours.

### Immunocytochemistry

Cells were fixed with 4% paraformaldehyde in phosphate-buffered saline (PBS) for 10 minutes on ice, permeabilized with 0.2% Triton X-100 in PBS for 5 minutes, and stained with rabbit anti-USP36 (1:1000), mouse anti-nucleolus (1:20; MAB1277, Millipore, Billerica, MA), mouse FK2 (1 μg/ml), mouse anti-NPM (10 μg/ml) and rabbit anti-Flag (0.4 μg/ml, Sigma) antibodies. Secondary antibodies were Alexa Fluor 488- and Alexa Fluor 594-conjugated anti-mouse IgG and anti-rabbit IgG antibodies (1:1000; Invitrogen, Carlsbad, CA). To stain nuclei, cells were incubated with TO-PRO-3 iodide (642/661) (50 μM, Invitrogen) or SYTOX green (1 μM, Invitrogen) during the incubation with secondary antibodies. Images were captured with a laser-scanning confocal microscope (Axiovert 200M, Carl Zeiss, Oberkochen, Germany) using the LSM5 PASCAL system (Carl Zeiss).

### Large-scale preparation of ubiquitylated proteins

Flag-USP36$^{C131A}$-transfected HeLa cells from ten 90-mm dishes were scraped into 4 ml of 10 mM Tris-HCl, pH 7.4, containing 10 mM N-ethylmaleimide and protease inhibitor cocktail, and homogenized by passing through a 23-gauge needle 15 times. Nuclei were precipitated by centrifugation at 1000 ***g*** for 5 minutes, and nuclear proteins were extracted from the nuclear pellet with 0.3 ml solubilizing buffer (50 mM Tris-HCl, pH 7.4, 300 mM NaCl, 0.5% Nonidet P-40, 1 mM EDTA, 10 mM N-ethylmaleimide and protease inhibitor cocktail). After centrifugation at 12,000 ***g*** for 15 minutes, the supernatant was incubated with anti-ubiquitin antibody FK2 (2 mg, Nippon Bio-Test, Kokubunji, Japan) conjugated to protein-A-Sepharose (1 ml, GE Healthcare) as described (Matsumoto et al., 2005) for 1 hour at 4°C. After washing the beads with solubilizing buffer, bound proteins were eluted with 100 mM glycine-HCl, pH 2.8, and neutralized with 1 M Tris-HCl, pH 8.0.

### Liquid chromatography and tandem mass spectroscopy

Ubiquitylated proteins purified from nuclei of USP36$^{C131A}$-transfected cells were reduced with dithiothreitol, alkylated with iodoacetamide and digested with trypsin as described (Matsumoto et al., 2005). The resulting peptides were separated into 18 fractions using cation-exchange chromatography (Polysulfoethyl A, PolyLC, Columbia, MD), and each fraction was subjected to reverse-phase chromatography on a $C_{18}$ column (L-column, Chemicals Evaluation and Research Institute, Saitama, Japan) with an HPLC system (Magic 2002, Michrom BioResources, Auburn, CA) that was coupled to an ion-trap mass spectrometer (Finnigan LCQ-Deca, Thermo Fisher Scientific, Waltham, MA) equipped with a nano-electrospray ionization source (AMR, Tokyo, Japan) as described (Matsumoto et al., 2005). Uninterpretable collision-induced dissociation spectra were compared with the Human International Protein Index ver. 3.1.6 (IPI, European Bioinformatics Institute) with the use of MASCOT algorithm. Mass tolerance for MS peaks and MS/MS peaks were 1.5 Da and 0.8 Da, respectively.

### Electron microscopy

For conventional EM, cells were cultured on plastic coverslips (Sumitomo Bakelite, Tokyo, Japan), and fixed in 2.5% glutaraldehyde in 0.1 M phosphate buffer, pH 7.4 (PB) for 2 hours. Cells were post-fixed in PB containing 1% $OsO_4$ and 1.5% potassium ferrocyanide for 1 hour, dehydrated in a series of graded ethanol solutions, and embedded in epoxy resin. Ultra-thin sections were observed under an H7600 electron microscope (Hitachi, Tokyo, Japan). For immuno-EM, the pre-embedding gold enhancement immuno gold method was performed as described (Luo et al., 2006)

with slight modification. Cells cultured on plastic cover glasses were fixed in 4% paraformaldehyde in PB for 20 minutes, and permeabilized in 0.25% saponin in PB for 30 minutes. After blocking in PB containing 0.1% saponin, 10% bovine serum albumin, 10% normal goat serum and 0.1% cold water fish skin gelatin, cells were incubated overnight with pre-immune serum or rabbit anti-USP36 antibody (1:200), then with colloidal gold (1.4 nm in diameter) conjugated with anti-rabbit IgG (Nanoprobes, NY) for 2 hours, and fixed in 1% glutaraldehyde in PB. Gold labeling was intensified with a gold enhancement kit (GoldEnhance EM, Nanoprobes, NY). Cells were post-fixed in PB containing 1% $OsO_4$ and 1.5% potassium ferrocyanide and processed as described for conventional EM.

### Metabolic labeling of rRNA

Cells were pre-incubated in phosphate-free medium (Invitrogen) supplemented with 0.5% fetal bovine serum for 30 minutes, then incubated in the same medium supplemented with 0.1 mCi/ml [$^{32}$P]orthophosphate (PerkinElmer, Wellesley, MA) for 45 minutes. Cells were washed twice with PBS, and incubated in the presence of 5% fetal bovine serum for the indicated duration. Total RNA was isolated from the cells using an RNA extraction kit (ISOGEN, Nippon Gene, Tokyo, Japan), separated by formaldehyde-denaturing agarose gel electrophoresis, and transferred to a nylon membrane. The membrane was exposed to an X-ray film to detect labeled RNA, then stained with 0.2 mg/ml methylene blue to detect loaded RNA. The radioactivity of rRNA bands was quantified using the BAS2000 Bio-Imaging Analyzer (Fujix, Tokyo, Japan).

### Ribosome profiling

Cells were treated with 0.36 mM CHX for 10 minutes, and harvested from culture dishes by trypsinization. An equal number of cells were homogenized by passage through a 23-gauge needle 40 times in 10 mM HEPES, pH 7.9, 10 mM KCl, 1.5 mM $MgCl_2$, 0.5 mM dithiothreitol and 0.36 mM CHX. The homogenates were centrifuged at 1000 ***g*** for 10 minutes, then twice at 12,000 ***g*** for 5 minutes at 4°C, and supernatants were collected as cytoplasmic fractions. Ribosome profiling of the fractions was performed as described (Inada and Aiba, 2005). Briefly, cytoplasmic fractions were layered onto linear 10-50% sucrose density gradients, and centrifuged at 136,000 ***g*** for 3 hours at 4°C. Gradients were fractionated, and ribosome profiles were generated by continuous absorbance measurement at 254 nm.

We thank E. Mizuno-Yamasaki for advice on the preparation of ubiquitylated proteins, and T. Suzuki and M. Tsujimoto for reagents. This work was supported by Grants-in-aid from the Ministry of Education, Culture, Sports, Science and Technology of Japan to M.K. (No. 19570178) and to N.K. and M.K. (No. 18657040).

## References

**Adachi, Y., Copeland, T. D., Hatanaka, M. and Oroszlan, S.** (1993). Nucleolar targeting signal of Rex protein of human T-cell leukemia virus type I specifically binds to nucleolar shuttle protein B-23. *J. Biol. Chem.* **268**, 13930-13934.

**Amerik, A. Y. and Hochstrasser, M.** (2004). Mechanism and function of deubiquitinating enzymes. *Biochim. Biophys. Acta* **1695**, 189-207.

**Andersen, J. S., Lam, Y. W., Leung, A. K., Ong, S. E., Lyon, C. E., Lamond, A. I. and Mann, M.** (2005). Nucleolar proteome dynamics. *Nature* **433**, 77-83.

**Arabi, A., Rustum, C., Hallberg, E. and Wright, A. P.** (2003). Accumulation of c-Myc and proteasomes at the nucleoli of cells containing elevated c-Myc protein levels. *J. Cell Sci.* **116**, 1707-1717.

**Bernstein, K. A., Bleichert, F., Bean, J. M., Cross, F. R. and Baserga, S. J.** (2007). Ribosome biogenesis is sensed at the Start cell cycle checkpoint. *Mol. Biol. Cell* **18**, 953-964.

**Blagoev, B., Kratchmarova, I., Ong, S. E., Nielsen, M., Foster, L. J. and Mann, M.** (2003). A proteomics strategy to elucidate functional protein-protein interactions applied to EGF signaling. *Nat. Biotechnol.* **21**, 315-318.

**Boisvert, F. M., van Koningsbruggen, S., Navascues, J. and Lamond, A. I.** (2007). The multifunctional nucleolus. *Nat. Rev. Mol. Cell. Biol.* **8**, 574-585.

**Chen, M., Rockel, T., Steinweger, G., Hemmerich, P., Risch, J. and von Mikecz, A.** (2002). Subcellular recruitment of fibrillarin to nucleoplasmic proteasomes: implications for processing of a nucleolar autoantigen. *Mol. Biol. Cell* **13**, 3576-3587.

**Fatica, A. and Tollervey, D.** (2002). Making ribosomes. *Curr. Opin. Cell Biol.* **14**, 313-318.

**Finley, D., Bartel, B. and Varshavsky, A.** (1989). The tails of ubiquitin precursors are ribosomal proteins whose fusion to ubiquitin facilitates ribosome biogenesis. *Nature* **338**, 394-401.

**Fujimuro, M. and Yokosawa, H.** (2005). Production of antipolyubiquitin monoclonal antibodies and their use for characterization and isolation of polyubiquitinated proteins. *Methods Enzymol.* **399**, 75-86.

**Grandori, C., Gomez-Roman, N., Felton-Edkins, Z. A., Ngouenet, C., Galloway, D. A., Eisenman, R. N. and White, R. J.** (2005). c-Myc binds to human ribosomal DNA and stimulates transcription of rRNA genes by RNA polymerase I. *Nat. Cell Biol.* **7**, 311-318.

**Grummt, I.** (1999). Regulation of mammalian ribosomal gene transcription by RNA polymerase I. *Prog. Nucleic Acid Res. Mol. Biol.* **62**, 109-154.

**Gustafson, W. C., Taylor, C. W., Valdez, B. C., Henning, D., Phippard, A., Ren, Y., Busch, H. and Durban, E.** (1998). Nucleolar protein p120 contains an arginine-rich domain that binds to ribosomal RNA. *Biochem. J.* **331**, 387-393.

**Haglund, K. and Dikic, I.** (2005). Ubiquitylation and cell signaling. *EMBO J.* **24**, 3353-3359.

**Hahn, M. A. and Marsh, D. J.** (2007). Nucleolar localization of parafibromin is mediated by three nucleolar localization signals. *FEBS Lett.* **581**, 5070-5074.

**Hernandez-Verdun, D.** (2006). Nucleolus: from structure to dynamics. *Histochem. Cell Biol.* **125**, 127-137.

**Hernandez-Verdun, D., Roussel, P. and Gebrane-Younes, J.** (2002). Emerging concepts of nucleolar assembly. *J. Cell Sci.* **115**, 2265-2270.

**Horke, S., Reumann, K., Schweizer, M., Will, H. and Heise, T.** (2004). Nuclear trafficking of La protein depends on a newly identified nucleolar localization signal and the ability to bind RNA. *J. Biol. Chem.* **279**, 26563-26570.

**Inada, T. and Aiba, H.** (2005). Translation of aberrant mRNAs lacking a termination codon or with a shortened 3′-UTR is repressed after initiation in yeast. *EMBO J.* **24**, 1584-1595.

**Itahana, K., Bhat, K. P., Jin, A., Itahana, Y., Hawke, D., Kobayashi, R. and Zhang, Y.** (2003). Tumor suppressor ARF degrades B23, a nucleolar protein involved in ribosome biogenesis and cell proliferation. *Mol. Cell* **12**, 1151-1164.

**Jans, D. A., Xiao, C. Y. and Lam, M. H.** (2000). Nuclear targeting signal recognition: a key control point in nuclear transport? *BioEssays* **22**, 532-544.

**Kim, M. S., Kim, Y. K., Kim, Y. S., Seong, M., Choi, J. K. and Baek, K. H.** (2005). Deubiquitinating enzyme USP36 contains the PEST motif and is polyubiquitinated. *Biochem. Biophys. Res. Commun.* **330**, 797-804.

**Lam, Y. W., Lamond, A. I., Mann, M. and Andersen, J. S.** (2007). Analysis of nucleolar protein dynamics reveals the nuclear degradation of ribosomal proteins. *Curr. Biol.* **17**, 749-760.

**Luo, H., Nakatsu, F., Furuno, A., Kato, H., Yamamoto, A. and Ohno, H.** (2006). Visualization of the post-Golgi trafficking of multiphoton photoactivated transferring receptors. *Cell Struct. Funct.* **31**, 63-75.

**Matsumoto, M., Hatakeyama, S., Oyamada, K., Oda, Y., Nishimura, T. and Nakayama, K. I.** (2005). Large-scale analysis of the human ubiquitin-related proteome. *Proteomics* **5**, 4145-4151.

**Mattsson, K., Pokrovskaja, K., Kiss, C., Klein, G. and Szekely, L.** (2001). Proteins associated with the promyelocytic leukemia gene product (PML)-containing nuclear body move to the nucleolus upon inhibition of proteasome-dependent protein degradation. *Proc. Natl. Acad. Sci. USA* **98**, 1012-1017.

**Nijman, S. M., Luna-Vargas, M. P., Velds, A., Brummelkamp, T. R., Dirac, A. M., Sixma, T. K. and Bernards, R.** (2005). A genomic and functional inventory of deubiquitinating enzymes. *Cell* **123**, 773-786.

**Oeffinger, M. and Tollervey, D.** (2003). Yeast Nop15p is an RNA-binding protein required for pre-rRNA processing and cytokinesis. *EMBO J.* **22**, 6573-6583.

**Peng, J., Schwartz, D., Elias, J. E., Thoreen, C. C., Cheng, D., Marsischky, G., Roelofs, J., Finley, D. and Gygi, S. P.** (2003). A proteomics approach to understanding protein ubiquitination. *Nat. Biotechnol.* **21**, 921-926.

**Quesada, V., Diaz-Perales, A., Gutierrez-Fernandez, A., Garabaya, C., Cal, S. and Lopez-Otin, C.** (2004). Cloning and enzymatic analysis of 22 novel human ubiquitin-specific proteases. *Biochem. Biophys. Res. Commun.* **314**, 54-62.

**Raska, I., Shaw, P. J. and Cmarko, D.** (2006). Structure and function of the nucleolus in the spotlight. *Curr. Opin. Cell Biol.* **18**, 325-334.

**Redman, K. L. and Rechsteiner, M.** (1989). Identification of the long ubiquitin extension as ribosomal protein S27a. *Nature* **338**, 438-440.

**Rockel, T. D., Stuhlmann, D. and von Mikecz, A.** (2005). Proteasomes degrade proteins in focal subdomains of the human cell nucleus. *J. Cell Sci.* **118**, 5231-5242.

**Sato, K., Hayami, R., Wu, W., Nishikawa, T., Nishikawa, H., Okuda, Y., Ogata, H., Fukuda, M. and Ohta, T.** (2004). Nucleophosmin/B23 is a candidate substrate for the BRCA1-BARD1 ubiquitin ligase. *J. Biol. Chem.* **279**, 30919-30922.

**Spence, J., Gali, R. R., Dittmar, G., Sherman, F., Karin, M. and Finley, D.** (2000). Cell cycle-regulated modification of the ribosome by a variant multiubiquitin chain. *Cell* **102**, 67-76.

**Stavreva, D. A., Kawasaki, M., Dundr, M., Koberna, K., Muller, W. G., Tsujimura-Takahashi, T., Komatsu, W., Hayano, T., Isobe, T., Raska, I. et al.** (2006). Potential roles for ubiquitin and the proteasome during ribosome biogenesis. *Mol. Cell. Biol.* **26**, 5131-5145.

**Tschochner, H. and Hurt, E.** (2003). Pre-ribosomes on the road from the nucleolus to the cytoplasm. *Trends Cell Biol.* **13**, 255-263.

**Valdez, B. C., Perlaky, L., Henning, D., Saijo, Y., Chan, P. K. and Busch, H.** (1994). Identification of the nuclear and nucleolar localization signals of the protein p120. *J. Biol. Chem.* **269**, 23776-23783.

**Yuan, X., Zhou, Y., Casanova, E., Chai, M., Kiss, E., Grone, H. J., Schutz, G. and Grummt, I.** (2005). Genetic inactivation of the transcription factor TIF-IA leads to nucleolar disruption, cell cycle arrest, and p53-mediated apoptosis. *Mol. Cell* **19**, 77-87.

**Zhang, Y., Wolf, G. W., Bhat, K., Jin, A., Allio, T., Burkhart, W. A. and Xiong, Y.** (2003). Ribosomal protein L11 negatively regulates oncoprotein MDM2 and mediates a p53-dependent ribosomal-stress checkpoint pathway. *Mol. Cell. Biol.* **23**, 8902-8912.